Journal of Materials Chemistry B

PAPER

View Article Online
View Journal

Cite this: DOI: 10.1039/c9tb02170a

A colorimetric and electrochemical dual-mode biosensor for thrombin using a magnetic separation technique†

Wen-Jing Guo,[a] Xiao-Yan Yang,[a] Zhen Wu[b] and Zhi-Ling Zhang *[a]

Received 4th October 2019,
Accepted 1st November 2019

DOI: 10.1039/c9tb02170a

rsc.li/materials-b

In general, protein detection relies primarily on enzyme-linked immunosorbent assays. Here, we constructed a colorimetric and electrochemical dual-mode biosensor for thrombin detection based on the mechanism of aptamer recognition. Magnetic nanobeads (MBs) were used as carriers for separation and enrichment to quickly capture thrombin (TB) in the complex matrix. Also, the combination of MBs and the magnetic electrode array (MEA) effectively avoided the poisoning of the electrode by biological samples. Furthermore, hybridization chain reaction (HCR) was indirectly used to achieve amplification of TB. A large number of horseradish peroxidases (HRPs) were coupled with the amplified long nucleic acid fragments. Based on the color and current response of the substrate TMB catalyzed by HRP, a dual-mode detection system for thrombin was established to ensure the accuracy of the test results. The method had a minimum resolution of 10 nM to the naked eye and an electrochemical detection limit as low as 0.35 nM. In addition, the sensor provided good anti-interference ability in a complex matrix and showed great potential to detect TB in complex samples.

1. Introduction

Proteins are important compounds that contribute to the make up of an organism, and are closely related to the normal operation of the body. Whether in biological science research, clinical diagnosis or quality testing, protein quantification is a very important task.[1–4] In previous reports, the specific recognition mechanism based on antigen–antibody was the most commonly used quantitative basis for protein quantification.[5–8] However, antibodies are difficult to prepare and modify, and are sensitive to temperature, which limits their application. Nucleic acid aptamer is a nucleic acid sequence with a targeting effect screened *via* systematic evolution of ligands by exponential enrichment (SELEX).[9,10] It has shown unique advantages in various biosensors, such as easy preparation, easy modification and so on.[11–14] In addition, some nucleic acid amplification strategies such as loop-mediated isothermal amplification (LAMP),[15] rolling circle amplification (RCA),[16] and hybridization chain reaction (HCR)[17] have been greatly favored by researchers in recent years. Compared to antibodies, aptamers with nucleic acid structure are more convenient to combine with these nucleic acid amplification strategies to achieve amplification of the detection signal. Among them, the nuclease-independent HCR has significant advantages.[18,19] After the initiator triggers the reaction, two different nucleic acid hairpins spontaneously react with each other driven by chemical entropy change.[20] HCR has the advantages of easy design and operation, and it has shown great application prospect in the field of biological imaging[21] and biological detection[22] as an effective signal amplification strategy.

Nevertheless, the interference of complex matrices in samples still poses a challenge to precise quantification of targets. Many studies have shown that the application of a magnetic separation technique can effectively solve this problem.[23–25] Magnetic nanobeads (MBs) have been widely used in magnetic separation techniques because of the rapid magnetic response.[26–28] In addition, the magnetic electrode array (MEA) can effectively capture magnetic composites on the surface of the electrode. In our previous research,[29] we found out that the combination of MBs and MEA could not only weaken the interference of the complex matrix, but also avoid the poisoning of the electrode by biological samples, which could significantly improve the sensitivity of the complex sample detection.

Thrombin is a serine protease that has both coagulation and anticoagulation effects. At present, researchers have developed different methods for the detection of thrombin, such as colorimetry,[30] electrochemistry[31] and fluorescence.[32] Generally speaking, a colorimetric sensor will produce intuitive color

[a] Key Laboratory of Analytical Chemistry for Biology and Medicine (Ministry of Education), College of Chemistry and Molecular Sciences, Wuhan University, Wuhan, 430072, P. R. China. E-mail: zlzhang@whu.edu.cn; Fax: +86-27-68754067; Tel: +86-27-68756759

[b] Hubei Collaborative Innovation Center for Advanced Organic Chemical Materials, Ministry of Education Key Laboratory for the Synthesis and Application of Organic Functional Molecules, College of Chemistry and Chemical Engineering, Hubei University, Wuhan, 430062, P. R. China

† Electronic supplementary information (ESI) available. See DOI: 10.1039/c9tb02170a

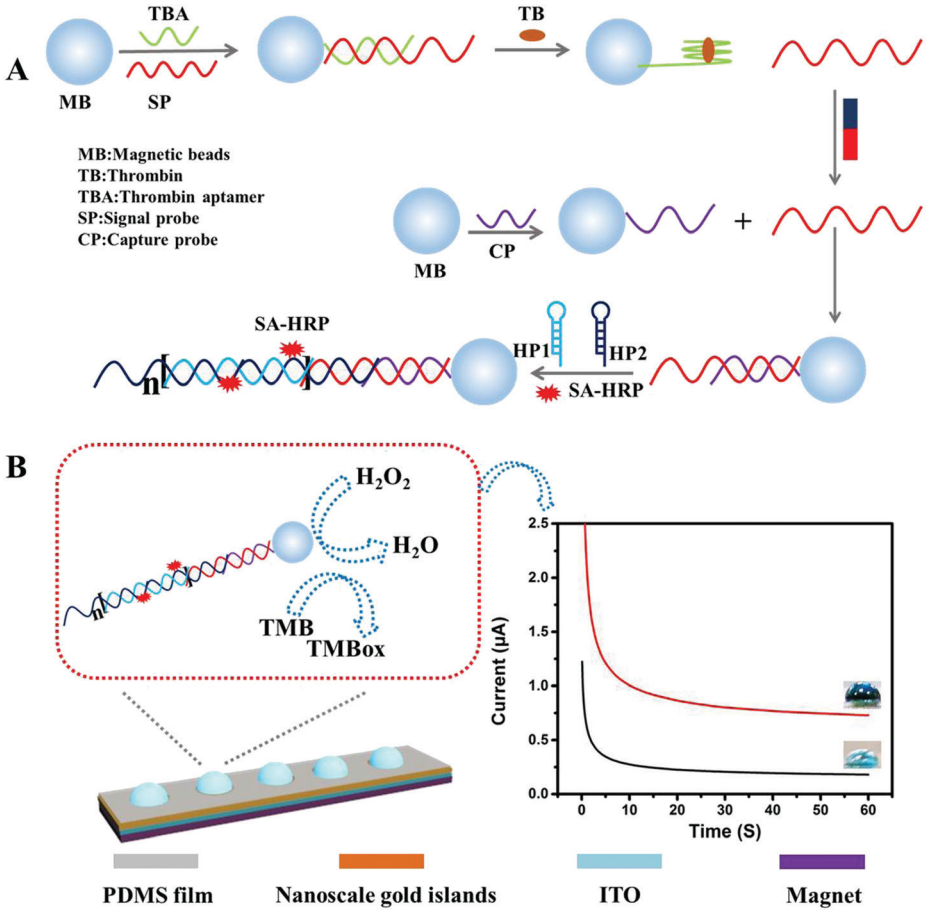

Scheme 1 Illustration of the protocol for electrochemical and colorimetric detection of thrombin: (A) capture of signal probe and HCR. (B) Colorimetric and electrochemical detection of thrombin on the same MEA.

changes visible to the naked eye, which is convenient to observe and obtain the detection information. Electrochemical sensors are popular because of their high sensitivity, low cost, simple operation and easy miniaturization. Based on the combination of the advantages of both, a kind of biosensor with dual signal output of colorimetry and electrochemistry emerges as the times require. Compared with the previous single-signal output sensor, the dual-signal output sensor can ensure the accuracy of the detection result and achieve accurate quantification of the target.

Here, we developed a colorimetric and electrochemical dual-mode sensor for thrombin detection based on HCR as a signal amplification strategy (Scheme 1). By utilizing the competitive binding of thrombin with the aptamer and its complementary strand of nucleic acid, the detection of the protein was converted to detection of its complementary strand of nucleic acid, facilitating the introduction of HCR indirectly to achieve amplification of thrombin. A large number of horseradish peroxidases (HRPs) were labeled on the amplified long chain nucleic acid through the specific action of biotin and streptavidin, which acted as a signal-labeled probe and had a remarkable enzymatic amplification effect. The MEAs were used for the capture of magnetic composites, effectively avoiding the poisoning of the electrodes by complex samples. Finally, the colorimetric and electrochemical dual-mode detection of thrombin was achieved by the colorimetric and electrochemical responses of the catalytic product of the enzyme in the pores of the array, respectively.

2. Experimental section

2.1. Chemicals and reagents

3,3′,5,5′-Tetramethylbenzidine (TMB) substrate solution was received from Thermo. Poly (dimethylsiloxane) (PDMS) was purchased from GE (GE Toshiba Silicones. Co., Ltd, Japan). *N*-(3-Dimethylaminopropyl)-*N*′-ethylcarbodiimide hydrochloride (EDC), trypsin, 2-(*N*-morpholino) ethanesulfonic acid (MES), thrombin (TB) from human plasma, $HAuCl_4$ and bovine serum albumin (BSA) were purchased from Sigma-Aldrich. Tris (hydroxymethyl) aminomethane (Tris) was purchased from Ruji. Biotechnology Co., Ltd, Shanghai. $NaH_2PO_4{\cdot}2H_2O$, $MgCl_2{\cdot}6H_2O$, $CaCl_2$, NaCl, $Na_2HPO_4{\cdot}12H_2O$, ethanol, and concentrated H_2SO_4 are analytically pure reagents, purchased from Sinopharm Chemical Reagent Co., Ltd (Shanghai, China). Horseradish peroxidase (HRP)-conjugated streptavidin (SA-HRP) and all the nucleic acid sequences purified by HPLC were purchased from

Shanghai Sangon Biotech (China), which were as follows: TBA: 5′-NH_2-TTTTTTTTGGTTGGTGTGGTTGG-3′; signal probe (SP): 5′-CCAACCACACCAACCAAAAAAAAAAAAAAAGTCTAGGATTCGGCG TGGGTTAA-3′; capture probe (CP): 5′-TTTTTTTTTTTTTGCTAG GTGTCGATGG-NH_2-3′; biotin-H1: 5′-TTAACCCACGCCGAATCC TAGACTCAAAGTAGTCTAGGATTCGGCGTG-biotin-3′; biotin-H2: 5′-AGTCTAGGATTCGGCGTGGGTTAACACGCCGAATCCTAGACTA CTTTG-biotin-3′.

2.2. Apparatus and measurements

All electrochemical tests including cyclic voltammetry, electrochemical impedance spectroscopy and chronoamperometry were performed by using a CHI660a electrochemical workstation (CH Instruments, Inc. Shanghai, China), using platinum wire as counter electrode and Ag/AgCl as reference electrode. UV-vis absorption spectra and fluorescence spectra were obtained from a UV-2550 (Shimadzu, Japan) spectrophotometer and a fluorescence spectrometer (Horiba Jobin Yvon), respectively. A smart phone (Honor 10, Huawei, China) was used to take colorimetric pictures. TEM (FEI Tecnai G2 20 TWIN) was used to obtain the morphology of magnetic nanobeads (MBs). SEM (ZEISS SIGMA FESEM) was used to characterize nanoscale gold islands.

2.3. Preparation of magnetic electrode array (MEA) modified by nanoscale gold islands

The nanoscale gold islands were prepared by the seed-growth synthesis method using ITO glass as the substrate according to the literature.[33] First of all, the ITO glass was cut into 1.5 × 1.5 cm^2 square pieces for preliminary cleaning, and then immersed in piranha solution (V/V, concentrated H_2SO_4/30% H_2O_2, 7 : 3) for about 5 min. After that, it was rinsed off with water and dried with N_2. A mixed solution of 4.3 mL of H_2O, 600 μL of 1% $HAuCl_4$ and 100 μL of $NH_3{\cdot}H_2O$ was used as the seed solution, and the treated ITO glass was placed into this solution, and gently shook for 5 minutes. Subsequently, the rinsed ITO glass was placed in 1 mM $NaBH_4$ and shaken slowly for 10 min. Finally, a mixed solution of 750 μM $HAuCl_4$ and $NH_2OH{\cdot}HCl$ was used as the growth solution. The above treated ITO glass was placed therein and slowly shaken for 5 min, and stood for 10 min. After rinsing and drying, the nanoscale gold islands could be prepared on the ITO substrate.

The proper amount of PDMS (w/w, RTV615A/RTV615B, 10/1) was evenly mixed and put on a silicon wafer. Then, PDMS was tiled on the surface of the silicon wafer (rotating speed: 600 rpm) by a spin coater and placed in an oven (75 °C) to form a PDMS film. A rectangular piece of 1.5 × 1 cm^2 of PDMS film with well-arranged holes of 2 mm was cut out. And then the ITO electrode array modified by nanoscale gold islands could be fabricated by covering the surfaces of ITO glass with the above PDMS film with holes. The MEA was prepared by placing a magnet at the bottom of the ITO glass.

2.4. Preparation of magnetic nanobeads (MBs)–thrombin aptamer(TBA)–signal probe (SP) complex

0.48 nM of the thrombin aptamer (TBA) and the signal probe (SP) were mixed evenly, and an appropriate amount of buffer solution was added to the mixed solution to make the total volume 50 μL. Then, it was placed in a PCR amplifier for annealing (95 °C for 5 min; 25 °C for 2 h) to form a complementary double-stranded TBA-SP, which was placed in a 4 °C refrigerator for storage.

According to previous reports of our group,[34,35] MBs were prepared by a layer-by-layer self-assembly method. 40 μL of MBs (15 mg mL^{-1}) was washed three times with MES buffer solution and dispersed in 100 μL of MES buffer solution. 4 mg of EDC was weighed and added into 100 μL of MES buffer solution, which was then rapidly added to the above MBs. Subsequently, 50 μL of TBA-SP and 150 μL of MES buffer were added, and reacted for 4 h in a 37 °C shaker with gentle shaking. After the reaction, it was washed three times with Tris–HCl buffer solution, and dispersed in 200 μL of Tris–HCl buffer solution containing 1% BSA at 4 °C for half an hour. Finally, after three cycles of washing, MBs–TBA–SP was placed in 200 μL of Tris–HCl buffer solution for further use.

Likewise, the preparation of the capture MBs (MBs–CP) was similar to the preparation of MBs–TBA–SP described above. Only 50 μL of TBA–SP was replaced by 50 μL of 9.5 μM capture probe (CP).

2.5. Colorimetric and electrochemical dual-mode detection of thrombin (TB)

40 μL of MBs-TBA-SP complex was mixed with different concentrations of TB and reacted for 2 h in a shaker (37 °C) with gentle shaking. The supernatant solution after magnetic adsorption was taken up and reacted with 20 μL of MBs-CP at 25 °C for 1 h. After removing the supernatant, 50 μL of 1 μM HP1 and 50 μL of 1 μM HP2 were added and reacted for 4 h in a shaker (25 °C). After washing several times to remove the unreacted hairpin nucleic acid, 100 μL of 1 μg mL^{-1} SA-HRP containing 1% BSA was added and reacted for 30 min at 37 °C in a shaker. After removing the excess enzyme by magnetic separation, the prepared magnetic composite was captured on the pores of the MEA, then 4 μL of TMB was added to each well. After reacting in a shaker for 10 min, the reaction was terminated by adding 1 μL of 0.5 M H_2SO_4. Finally, the photos were taken by using a mobile phone. In the traditional three-electrode system, MEA was used as the working electrode, Ag/AgCl was the reference electrode and platinum wire was the opposite electrode. The parameters of the chronoamperometric method are set to the potential of 100 mV, the sweep speed of 0.1 V s^{-1}, and the time of 60 s.

3. Results and discussion

3.1. Characterization of magnetic electrode array (MEA) modified by nanoscale gold islands

Nanoscale gold islands were prepared on ITO glass by a seed-growth synthesis method (Fig. 1A). Based on the adjustment of pH by ammonia, $AuCl^{4-}$ was deposited on the surface of ITO glass substrates and further reduced to Au^0 by $NaBH_4$. After the further reduction of $AuCl^{4-}$ by hydroxylamine, Au^0 of small size grew into nanoscale gold islands. SEM was used to characterize the surface morphology of the nanoscale gold islands, which showed a uniform single-layer island distribution (Fig. 1B). The nanoscale

gold island-modified MEA was prepared by covering a PDMS film with an array of small holes. The cyclic voltammetry curves of the electrodes of MEA in 0.5 M H_2SO_4 had obvious redox peaks of gold, which proved the successful modification of nanoscale gold islands on ITO glass (Fig. 1C). According to the peak charge obtained by cyclic voltammetry scanning, the electroactive area of an electrode of MEA was calculated to be 2.44 mm^2. The electroactivity of the electrode array was further characterized by cyclic voltammetry scanning of 5 randomly selected independent electrodes in 0.5 M H_2SO_4 (Fig. 1D), demonstrating the uniform electrical activity of MEA. In addition, electrochemical impedance spectroscopy (EIS) showed that the impedance of the electrode modified by nanoscale gold islands was much smaller than that of the unmodified electrode (Fig. 1E). The above results indicated that the MEA with good performance could be further used for subsequent detection.

3.2. Characterization of magnetic nanobeads (MBs)

In clinical diagnosis, the interference of complex matrix is a non-negligible problem. MBs could be used as effective tools to quickly realize the capture of target substances in complex samples, which can effectively weaken the effects of complex matrix. Here, MBs were prepared by the layer-by-layer self-assembly method developed by our group,[31,32] and the performance of MBs was characterized by TEM. Fig. 2A showed that MBs with a size of approximately 310 nm had good monodisperse properties. According to the capture amount of MBs by commercial magnetic scaffold at different times, the capture efficiency–time curve was obtained (Fig. 2C). The results showed that almost all the MBs could be captured by the magnetic scaffold within 2 minutes. MBs with a fast magnetic response offer the possibility of detection in complex samples.

3.3. Characterization of MBs–thrombin aptamer (TBA)–signal probe (SP) complex and MBs–capture probe (CP) complex

Based on the principle of complementary base pairing, TBA and SP form TBA–SP double stranded nucleic acid. The surface of MBs was rich in carboxyl groups, which could be used for coupling of aptamers with amino groups at the 5′ end. The alexa-488 dye produces green fluorescence under blue light excitation. Therefore, SP with alexa-488 label at the 3′ end was used to verify the success of the coupling reaction between MBs

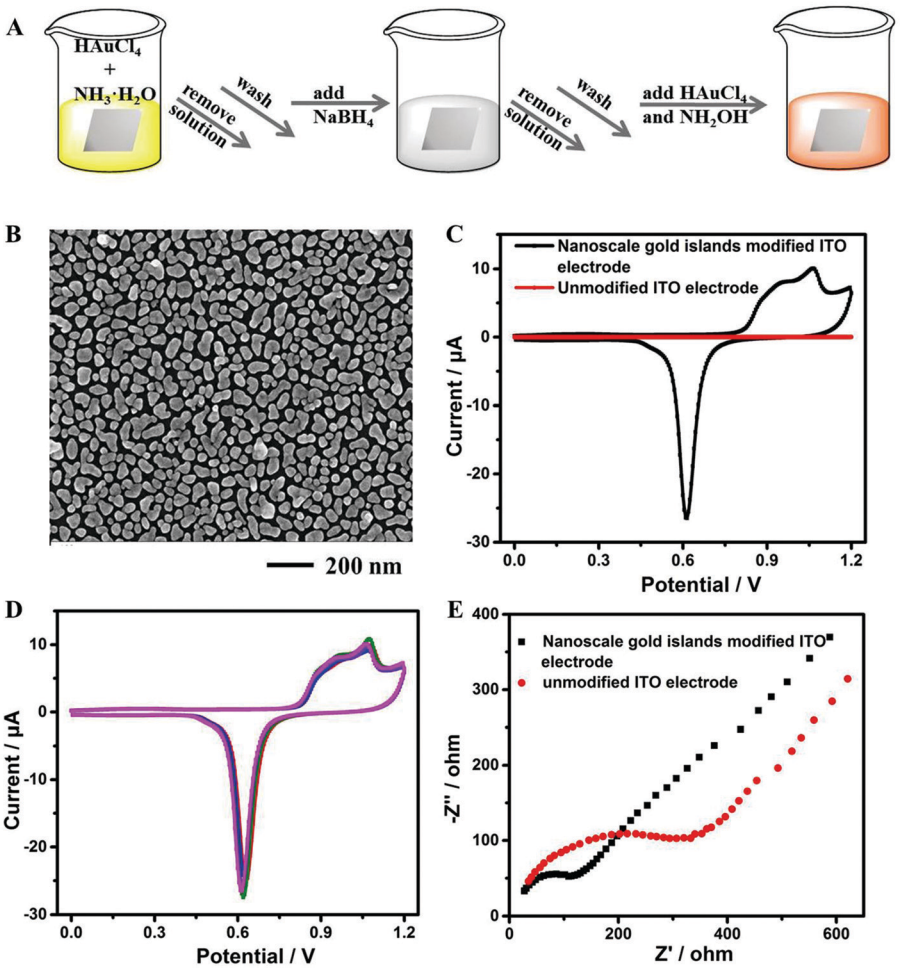

Fig. 1 (A) Fabrication of nanoscale gold islands on ITO glass. (B) SEM image of nanoscale gold islands on ITO glass. (C) Cyclic voltammetry curves of a nanoscale gold island-modified electrode and an unmodified electrode in 0.5 M H_2SO_4. (D) Cyclic voltammetry curves of five nanoscale gold island-modified electrodes in 0.5 M H_2SO_4. (E) Electrochemical impedance spectroscopy (EIS) of a nanoscale gold island-modified electrode and an unmodified electrode.

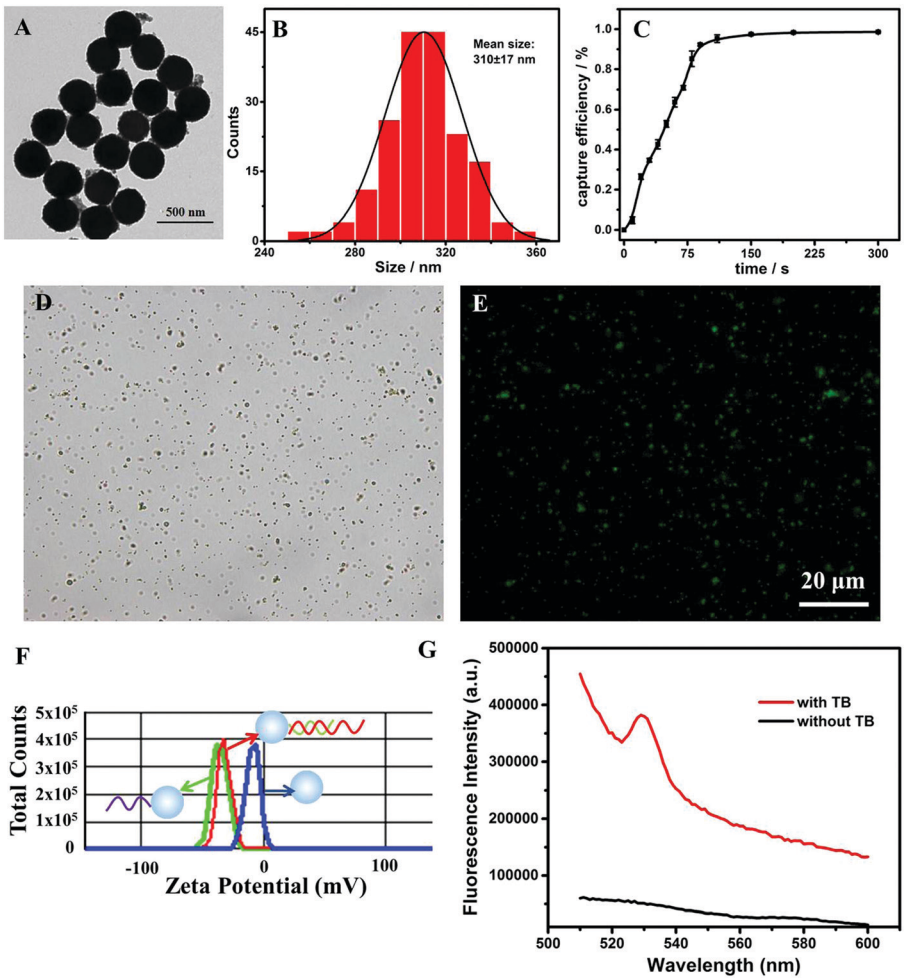

Fig. 2 (A) TEM image of MBs. (B) Size distribution of MBs. (C) Magnetic response test of MBs with a commercial magnetic scaffold. (D) Microscopic images of MBs–TBA–SP (bright field). (E) Microscopic images of MBs–TBA–SP (fluorescence field). (F) Zeta potential of MBs and MBs after reacting with TBA–SP or CP. (G) Fluorescence spectra of the supernatant after the reaction between MBs–TBA–SP and TB or without TB.

and TBA–SP (Fig. 2D and E). In addition, the negative shift of zeta potential further indicates the successful coupling of MBs and TBA–SP or CP (Fig. 2F).

The number of aptamers on the surface of MBs was very important for efficient capture of the target, which was also determined by using the SP with the alexa-488 tag at the 3′ end. Based on ultraviolet absorption of MBs, the standard curve of MBs was drawn (Fig. S1A, ESI†), and the standard curve of SP with alexa-488 at the 3′ end was plotted by UV photometry and fluorescence spectroscopy (Fig. S1B and C, ESI†). After calculation, an average of 108 nucleic acid aptamers were coupled to the surface of each MB and contributed to the capture of thrombin (TB). After the MBs–TBA–SP complex was incubated with TB for a certain time, the fluorescence of the SP with alexa-488 at the 3′ end in the supernatant after magnetic separation could be detected by a fluorescence spectrometer (Fig. 2G), which demonstrated that SP was successfully replaced by a competing binding of the aptamer to thrombin.

3.4. Feasibility of the biosensor for TB detection

Based on the combination of a magnetic separation technique with hybridization chain reaction (HCR) as an amplification strategy, a colorimetric and electrochemical dual-mode method was developed. In order to verify the feasibility of the method, four sets of controlled trials were designed (Fig. 3). The developed

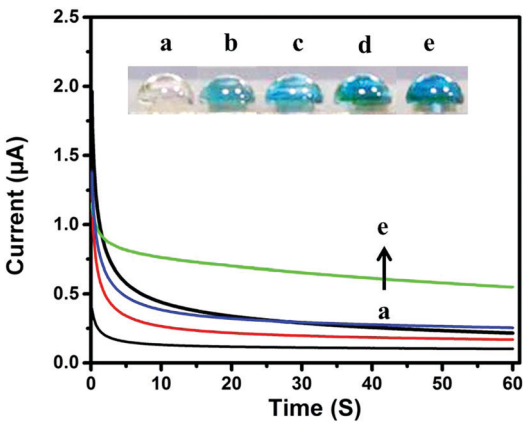

Fig. 3 Chronoamperometric responses of different conditions (a) without SA–HRP, (b) without signal probe, (c) without TB, (d) without biotin–H2, and (e) with TB (The inset is the corresponding colorimetric picture).

sensor used horseradish peroxidase (HRP) as a label to achieve detection signal. Under the catalysis of HRP, TMB was oxidized to form a colored bisazobenzidine. Without HRP, there was a weak current response and a nearly transparent color (Fig. 3a). In the absence of SP or TB, a weak current and small color change were obtained (Fig. 3b and c), indicating that MBs-CP could not capture SP for the next HCR. As shown in Fig. 3b–d, the weak signal output is due to non-specific adsorption of the enzyme, but it could still be distinguished from the experimental group. Without biotin-H2, HCR did not occur (Fig. 3d). As an effective signal amplification strategy, HCR could significantly enhance the signal. Obvious colorimetric and electrochemical signals distinct from the background signals could only be observed in the experimental group (Fig. 3e) where all substances are present. The results showed that the developed sensor could be used for TB detection.

3.5. Colorimetric and electrochemical dual-mode detection of TB

Under the optimal detection conditions, the developed biosensor was used for colorimetric and electrochemical dual-mode detection of TB (Fig. 4A). As the concentration of TB increases, the number of replaced SP increases, which could be captured by MBs-CP, and amplified by HCR to provide a large number of labeling sites. Based on the specific recognition of biotin and avidin, a large amount of HRP could be coupled to the nucleic acid polymer and catalyze the color development of the substrate. In summary, the higher the concentration of TB, the deeper the color of the solution, and the stronger the electrochemical signal. In addition, the use of MEA contributed to the capture of the magnetic complex, thereby obtaining a direct color development effect of multiple samples, which was more convenient and intuitive. As shown in Fig. 4A, the colorimetric signal produced by as little as 10 nM TB could be obtained. It was observed that the current increased as the concentration of the target increased (Fig. 4B and C). In the concentration range of 1 nM to 10 μM, the current intensity and the logarithmic concentration of TB showed a good linear relationship with a detection limit as low as 0.35 nM (S/N = 3). In addition, compared to other methods (Table S1, ESI†), this method is based on a pattern in which one reporter produced a colorimetric and electrochemical dual signal, which ensured the accuracy of the test results.

In general, the sensor's superior performance was attributed to the following: (1) the use of MBs facilitated the capture of targets in complex systems, reducing the impact of complex matrices. (2) The detection of thrombin was converted into detection of SP, which was convenient to introduce HCR to achieve amplification. (3) The developed sensor was based on the colorimetric and electrochemical dual output signal mode to ensure the accuracy of the test results.

The specificity of the method was examined using the same concentration of trypsin, bovine serum albumin (BSA), histidine (His) and thrombin. As shown in Fig. 5, unlike other substances, TB produced a more notable current response, causing a more pronounced color change, which indicated that the method had strong specificity to specifically detect TB.

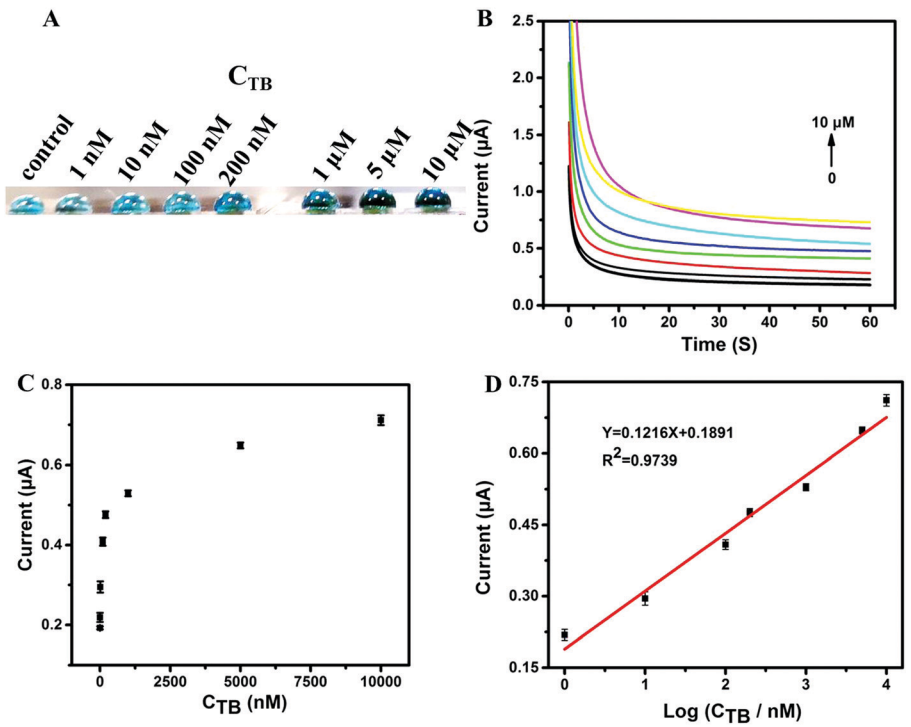

Fig. 4 (A) Colorimetric detection of thrombin under different concentrations of thrombin. (B) Electrochemical detection of TMB under different concentrations of thrombin (0, 1 nM, 10 nM, 100 nM, 200 nM, 1 μM, 5 μM, and 10 μM). (C) The plot of current intensity *vs.* the concentration of thrombin. (D) Linear curve between currents and the concentration of thrombin.

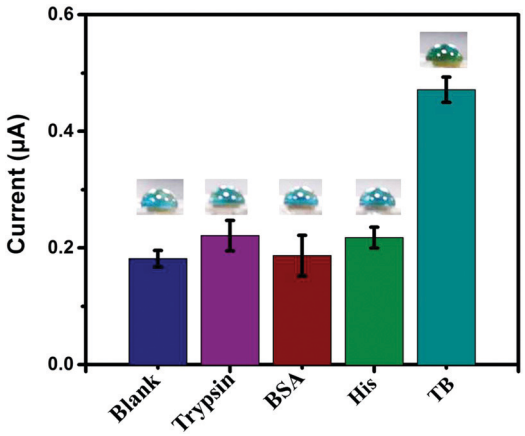

Fig. 5 The developed biosensor for detection of blank, trypsin, BSA, His and TB with the same concentration of 200 nM.

Table 1 Determination of thrombin by the standard addition method in human serum

Samples	Added (nM)	Found (nM)	Recovery (%)	RSD (%)
1	10	9.76	97.6	3.6
2	200	207.60	103.8	4.5

3.6. Detection of TB in human serum

In clinical diagnosis, the interference of complex matrices became a huge obstacle to the detection of the target. In order to evaluate the applicability of the sensor in complex samples, we performed electrochemical detection of thrombin in a 1% human serum system using standard addition methods. Human serum samples were taken from Zhongnan Hospital of Wuhan University. As shown in Table 1, the method could obtain a spike recovery of 97.6–103.8%, which proved that the method still exhibited good anti-interference ability in complex samples and could be applied to the detection of TB in complex samples.

4. Conclusions

In summary, we constructed a colorimetric and electrochemical dual-mode sensor for the detection of TB based on HCR as a signal amplification strategy. With the amplification of HCR, the electrochemical and colorimetric signal was significantly enhanced. The colorimetric and electrochemical dual signal output methods ensure the accuracy of the test results. The colorimetric method detects a minimum of 10 nM and the electrochemical method has a detection limit as low as 0.35 nM. The application of MBs and MEA not only avoided the poisoning of the electrode by the biological sample, but also realized the simultaneous measurement of multiple sets of samples. The method had high sensitivity and specificity, and provided a route for the detection of TB in complex samples, which has potential advantages in the early diagnosis of diseases.

Conflicts of interest

There are no conflicts to declare.

Acknowledgements

This work was supported by the National Natural Science Foundation of China (21775111) and the National Science and Technology Major Project of China (2018ZX10301405).

References

1 O. H. Lowry, N. J. Rosebrough, A. L. Farr and R. J. Randall, *J. Biol. Chem.*, 1951, **193**, 265–275.
2 D. Baker and A. Sali, *Science*, 2001, **294**, 93–96.
3 G. Sina, H. Won-Ki, B. Kiowa, W. H. Russell, B. Archana, D. Noah, K. O. S. Erin and S. W. Jonathan, *Nature*, 2003, **425**, 737–741.
4 H. Arai, S. Higuchi and H. Sasaki, *Gerontology*, 1997, **43**, 2–10.
5 Z. B. Luo, Q. G. Qi, L. J. Zhang, R. J. Zeng, L. S. Su and D. P. Tang, *Anal. Chem.*, 2019, **91**, 4149–4156.
6 Z. A. Hu, G. W. Sun, W. C. Jiang, F. J. Xu, Y. Q. Zhang, M. C. Xia, X. Y. Pan, Z. Xing, S. C. Zhang and X. R. Zhang, *Anal. Chem.*, 2019, **91**, 5980–5986.
7 A. Sedighi and U. J. Krull, *Anal. Chem.*, 2019, **91**, 5371–5379.
8 Z. Z. Yu, Y. Tang, G. N. Cai, R. R. Ren and D. P. Tang, *Anal. Chem.*, 2019, **91**, 1222–1226.
9 A. D. Ellington and J. W. Szostak, *Nature*, 1990, **346**, 818–822.
10 C. Tuerk and L. Gold, *Science*, 1990, **249**, 505–510.
11 B. Wei, K. Mao, N. Liu, M. Zhang and Z. G. Yang, *Biosens. Bioelectron.*, 2018, **121**, 41–46.
12 I. Andrea, G. Julian, P. Claudio, K. Tod and W. P. Kevin, *Anal. Bioanal. Chem.*, 2019, **411**, 4629–4635.
13 H. F. Xu, F. X. Kou, H. Z. Ye, Z. W. Wang, S. X. Huang, X. X. Liu, X. Zhu, Z. Y. Lin and G. N. Chen, *Talanta*, 2017, **175**, 177–182.
14 A. S. Emrani, N. M. Danesh, P. Lavaee, M. Ramezani, K. Abnous and S. M. Taghdisi, *Food Chem.*, 2016, **190**, 115–121.
15 Y. Yuan, S. Wei, G. Liu, S. Xie, Y. Chai and R. Yuan, *Anal. Chim. Acta*, 2014, **811**, 70–75.
16 B. Veigas, J. Pinto, R. Vinhas, T. Calmeiro, R. Martins, E. Fortunato and P. V. Baptista, *Biosens. Bioelectron.*, 2017, **91**, 788–795.
17 D. D. Xu, C. Liu, C. Y. Li, C. Y. Song and H. W. Tang, *ACS Appl. Mater. Interfaces*, 2017, **9**, 37606–37614.
18 Z. L. Qiu, J. Shu, J. F. Liu and D. P. Tang, *Anal. Chem.*, 2019, **91**, 1260–1268.
19 B. Zhang, B. Q. Liu, D. P. Tang, R. Niessner, G. N. Chen and D. Knopp, *Anal. Chem.*, 2012, **84**, 5392–5399.
20 R. M. Dirks and N. A. Pierce, *Proc. Natl. Acad. Sci. U. S. A.*, 2004, **101**, 15275–15278.
21 Z. Wu, G. Q. Liu, X. L. Yang and J. H. Jiang, *J. Am. Chem. Soc.*, 2015, **137**, 6829–6836.
22 C. Jonghoon, L. Kerry Routenberg, G. Yuan, T. M. Gierahn and L. J Christopher, *Anal. Chem.*, 2011, **83**, 6890–6895.
23 M. K. Li, L. Y. Hu, C. G. Niu, D. W. Huang and G. M. Zeng, *Sens. Actuators, B*, 2018, **266**, 805–811.

24 Z. Wu, J. Hu, T. Zeng, Z. L. Zhang, J. J. Chen, G. Wong, X. G. Qiu, W. J. Liu, G. F. Gao, Y. H. Bi and D. W. Pang, *Anal. Chem.*, 2017, **89**, 2039–2048.
25 J. D. Wang, S. Y. Tan, Q. L. Liang, H. Y. Guan, Q. Han and M. Y. Ding, *Talanta*, 2019, **204**, 792–801.
26 C. H. Zhou, J. Y. Zhao, D. W. Pang and Z. L. Zhang, *Anal. Chem.*, 2014, **86**, 2752–2759.
27 M. Wu, Z. L. Zhang, G. Chen, C. Y. Wen, L. L. Wu, J. Hu, C. C. Xiong, J. J. Chen and D. W. Pang, *Small*, 2015, **11**, 5280–5288.
28 P. L. Guo, M. Tang, S. L. Hong, X. Yu, D. W. Pang and Z. L. Zhang, *Biosens. Bioelectron.*, 2015, **74**, 628–636.
29 C. H. Zhou, Y. M. Long, B. P. Qi, D. W. Pang and Z. L. Zhang, *Electrochem. Commun.*, 2013, **31**, 129–132.
30 L. Li, Y. Liang, Y. Zhao and Z. Chen, *Sens. Actuators, B*, 2018, **262**, 733–738.
31 Y. H. Wang, X. X. He, K. M. Wang, X. Q. Ni, J. Su and Z. Chen, *Biosens. Bioelectron.*, 2011, **26**, 3536–3541.
32 S. Umrao, V. Jain, S. Anusha, B. Chakraborty and R. Roy, *Sens. Actuators, B*, 2018, **267**, 294–301.
33 S. M. Tabakman, Z. Chen, H. S. Casalongue, H. L. Wang and H. J. Dai, *Small*, 2011, **7**, 499–505.
34 C. Y. Wen, L. L. Wu, Z. L. Zhang, Y. L. Liu, S. Z. Wei, J. Hu, M. Tang, E. Z. Sun, Y. P. Gong and J. Yu, *ACS Nano*, 2014, **8**, 941–949.
35 C. Y. Wen, J. Hu, Z. L. Zhang, Z. Q. Tian, G. P. Ou, Y. L. Liao, Y. Li, M. Xie, Z. Y. Sun and D. W. Pang, *Anal. Chem.*, 2013, **85**, 1223–1230.

